MECHANICAL PERFORMANCE OF ALLOY STEELS, NICKEL-SUPERALLOYS, AND TITANIUM IN HIGH-PERFORMANCE BALL BEARINGS

[1]ABDULLAH MOAFA, [2]PAOLO PENNACCHI

[1]Department of Mechanical Engineering, Politecnico di Milano Via Privata Giuseppe La Masa, 1, 20156 Milan, Italy.
E-mail: amoafa@tvtc.gov.sa

Abstract - This study investigates the mechanical performance of ball bearing inner and outer raceways made from alloy steels, nickel-based superalloys, and titanium alloys under varying applied loads and rotational speeds. Key parameters analysed include load-deflection constants, normal contact load, and fatigue life at rotational speeds ranging from 6,000 to 15,000 RPM and applied loads up to 47,500 N. The results reveal that alloy steels consistently exhibit the highest load-deflection resistance, indicating superior stiffness, while titanium alloys offer the greatest fatigue life under low-load conditions. However, the fatigue life of titanium degrades more rapidly with increased load and speed compared to the other materials. Normal contact loads increase with both load and speed for all materials, with alloy steels again demonstrating the highest values. These findings highlight the trade-offs between stiffness and endurance across different materials, offering insights for optimized material selection in high-performance bearing applications.

Keywords - Ball Bearings; Load-Deflection; Fatigue Life; Rotational Speed; Bearing Materials

I. INTRODUCTION

Ball bearings are key rotating machine components, providing low-friction support and precise load transfer between moving components. Their operational efficiency has direct implications for the reliability, efficiency, and lifespan of mechanical assemblies across a wide range of industries and applications, including automotive, aerospace, power generation, and manufacturing. The mechanical behaviour of a bearing—that is, the ability to resist distortion, transfer contact loads, and sustain cyclic stresses—depends to a large extent upon the raceway and rolling element material properties[1].

Some of the most critical parameters governing the behaviour of the bearing are the load-deflection constant, a structural stiffness measure of the bearing; the normal contact load, an indication of pressure transferred through areas of contact; and the fatigue life, governing the working life of the bearing under cyclic loading. The parameters are acutely sensitive to the extent of the applied load and the velocity of the bearing, given the greater velocities have the potential to exert higher centrifugal forces and thermal effects with the capacity to cause accelerated wear and failure[2].

Choice of material is important to optimize these factors of performance. Alloy steel has long been the traditional choice for its strength, hardness, and abrasion resistance. New engineering needs have replaced it with other metals such as nickel superalloys with desirable thermal properties and titanium alloys with high strength/weight ratio and corrosion resistance. These all possess a specific combination of mechanical and physical properties that can significantly affect the behaviour of the bearings under dynamic operating conditions[3].

The goal of the investigation is to contrast the properties - load-deflection constant, normal contact load, and fatigue life - of the ball raceway components of the three classes of alloys: the alloy steels, the nickel superalloys, and the titanium alloys when subjected to various loads and rotating speeds. The investigation through systematic testing of the test samples across the representative operating range is intended to provide useful guidelines to the designer and the engineer for the optimum selection of the most appropriate material for the intended application of the bearing, particularly for high-performance and mission-critical use.

II. THEORETICAL ANALYSIS

Roller and ball bearings support loads with rotational and translational movement. Unlike hydrodynamic bearings, rolling bearings have complex inner dynamics, e.g., element and shaft rotation, orbital movement, and sliding contact. Non-zero contact angles at high-speed produce spinning, gyroscopic effects, and greater inner speeds—especially for lubricated angular contact ball bearings[4]. These increase the centrifugal forces and the gyroscopic moment's effect on inner forces and deflection and stiffening the supported-load distribution. This chapter derives a model of such inner dynamics: the action of skidding, centrifugal forces, and the gyroscopic motion. Simplifying assumptions, i.e., "outer raceway control" and distribution of the gyroscopic moment, are made to compute inner forces and deflection economically under high-speed, thrust-loaded running.The model below is derived from [4-6].

2.1. Dynamic model for High-speed conditions

The radius of the locus of inner raceway groove curvature centersR_i is written in the following formula:

$$R_i = \frac{d_m}{2} + (r_i - 0.5D)\cos\alpha^o \text{ Eq.1}$$

Where α^o is the initial contact angle before loading. Additionally, the axial distance between the locations of the inner and outer raceway groove curvature centers at any ball position is determined by the relative angular displacements θ, and the relative axial displacement of the inner and outer rings,δ_a.

$$A_{1j} = BD\sin\alpha^\circ + \delta_a + \theta R_i \cos\psi_j \text{ Eq.2}$$

The radial displacement between the loci of the groove curvature centers at each ball location in accordance with a relative radial displacement of the ring centers δ_r is as follows:

$$A_{2j} = BD\cos\alpha^\circ + \delta_r \cos\psi_j \text{ Eq.3}$$

$$\cos\alpha_{oj} = \frac{X_{2j}}{(f_o - 0.5)D + \delta_{oj}} \text{ Eq.4}$$

$$\sin\alpha_{oj} = \frac{X_{1j}}{(f_o - 0.5)D + \delta_{oj}} \text{ Eq.5}$$

$$\cos\alpha_{ij} = \frac{A_{2j} - X_{2j}}{(f_i - 0.5)D + \delta_{ij}} \text{ Eq.6}$$

$$\sin\alpha_{ij} = \frac{A_{1j} - X_{1j}}{(f_i - 0.5)D + \delta_{ij}} \text{ Eq.7}$$

Considering the force balance in the vertical and horizontal axesas shown in Fig. 1,It can be found by using the Pythagorean theorem Fig.2 the following equations:

$$\left(A_{1j} - X_{1j}\right)^2 + \left(A_{2j} - X_{2j}\right)^2 - \left[(f_i - 0.5)D + \delta_{ij}\right]^2 = 0 \text{ Eq.8}$$

$$X_{1j}^2 + X_{2j}^2 - \left[(f_o - 0.5)D + \delta_{oj}\right]^2 = 0 \quad \text{Eq.9}$$

$$Q_{ij}\sin\alpha_{ij} - Q_{oj}\sin\alpha_{oj} - \frac{M_{gj}}{D}\left(\lambda_{ij}\cos\alpha_{ij} - \lambda_{oj}\cos\alpha_{oj}\right) = 0 \text{ Eq.10}$$

$$Q_{ij}\cos\alpha_{ij} - Q_{oj}\cos\alpha_{oj} + \frac{M_{gi}}{D}\left(\lambda_{ij}\sin\alpha_{ij} - \lambda_{oj}\sin\alpha_{oj}\right) + F_{cj} - G\sin\psi_j = 0 \text{ Eq.11}$$

Once values for δ_a, δ_r and θ are assumed, equations can be solved simultaneously for X_{1j}, X_{2j}, δ_{ij}, and δ_{oj} at each ball angular point. The Newton-Raphson method is the most likely approach of solving simultaneous nonlinear equations.

Knowing F_a, F_r and ω as input conditions, equations can be used to estimate the values ofδ_a, δ_r and θ using the computed values of X_{1j}, X_{2j}, δ_{ij} and δ_{oj} at each ball location. Once the fundamental unknown quantities δ_a, δ_r and θ have been determined, the calculations for of X_{1j}, X_{2j}, δ_{ij} and δ_{oj} and so forth must be repeated until the primary unknown quantities δ_a, δ_r and θ have compatible values. At equilibrium:

$$F_a - \sum_{j=1}^{j=Z}\left(\frac{K_{ij}\left(A_{1j} - X_{1j}\right)\delta_{ij}^{1.5} - \frac{\lambda_{ij}M_{gi}}{D}\left(A_{2j} - X_{2j}\right)}{(f_i - 0.5)D + \delta_{ij}}\right) = 0 \text{ Eq.12}$$

$$F_r - \sum_{j=1}^{j=Z}\left(\frac{K_{ij}\left(A_{2j} - X_{2j}\right)\delta_{ij}^{1.5} + \frac{\lambda_{ij}M_{gi}}{D}\left(A_{1j} - X_{1j}\right)}{(f_i - 0.5)D + \delta_{ij}}\right) = 0 \text{ Eq.13}$$

$$\mathfrak{M} - \sum_{j=1}^{j=Z}\left(\frac{K_{ij}\left(A_{1j} - X_{1j}\right)\delta_{ij}^{1.5} - \frac{\lambda_{ij}M_{gi}}{D}\left(A_{2j} - X_{2j}\right)\mathfrak{R}_i}{(f_i - 0.5)D + \delta_{ij}} + \lambda_{ij}f_i M_{gi}\right) \times \left[\cos\psi_j\right] = 0 \text{ Eq.14}$$

The load-deflection "constants" K_i and K_o in these equations, which can be solved iteratively, are functions of λ_i and λ_o, which are functions of X_1 and X_2.

$$Q_{i,oj} = K_{i,oj}\,\delta_{i,oj}^{1.5} \text{ Eq.15}$$

$$K_{o,i} = \frac{2\sqrt{2}\left(\frac{E}{1-\nu^2}\right)}{3(\sum\rho)^{1/2}}\left(\frac{1}{\delta^*}\right)^{\frac{3}{2}} \text{ Eq.16}$$

Where $\omega_m^2 = \left(\frac{\omega_m}{\omega}\right)^2\omega^2$, the centrifugal force is obtained as:

$$F_{cj} = \frac{1}{2}md_m\omega^2\left(\frac{\omega_m}{\omega}\right)_j^2 \text{ Eq.17}$$

$$M_{gj} = J\left(\frac{\omega_R}{\omega}\right)_j\left(\frac{\omega_m}{\omega}\right)_j\omega^2\sin\beta \text{ Eq.18}$$

$$\tan\beta = \frac{\sin\alpha_o}{\cos\alpha_o + \gamma'} \text{ Eq.19}$$

$$\gamma' = \frac{D}{d_m} \text{ Eq.20}$$

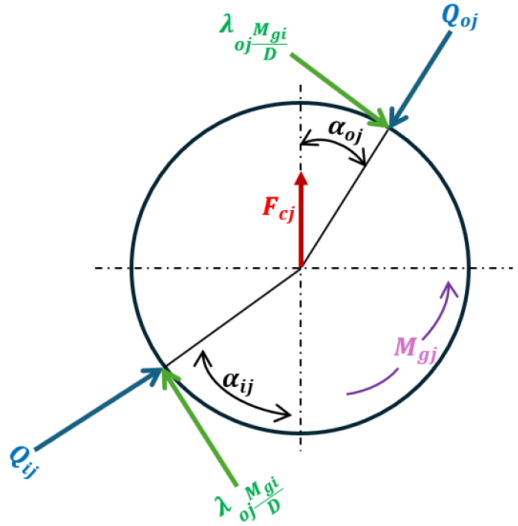


Fig. 1 Loaded ball at angular position ψ_j.

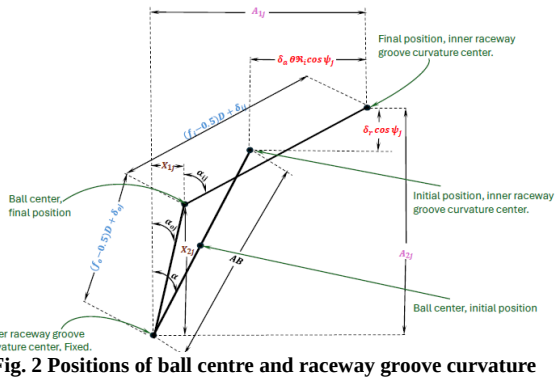


Fig. 2 Positions of ball centre and raceway groove curvature centres at angular position ψ, with and without applied load.

2.2. Bearing fatigue life calculation modelling

According to the foregoing analysis, the fatigue life of a rolling element- raceway point contact subjected to normal load $\boldsymbol{Q}$ may be estimated by[7]:

$$L = \left(\frac{Q_c}{Q}\right)^3 \quad \text{Eq. 21}$$

$$Q_{ci,o} = 93.2 * \left(\frac{2f_{i,o}}{2f_{i,0}-1}\right)^{0.41} \frac{(1-\gamma_{i,o})^{1.39}}{(1+\gamma_{i,o})^{1/3}} \left(\frac{\gamma_{i,o}}{cos\ \alpha_{i,o}}\right)^{0.3} D^{1.8} Z^{\frac{-1}{3}} \quad \text{Eq. 22}$$

To account for spinning, the inner raceway capacity is reduced by a factor of $1 - 0.33 \times \sin \alpha_i$.

$$L_{i,o} = \left(\frac{Q_{ci,o}}{Q_{ei,o}}\right)^3 \quad \text{Eq. 23}$$

$$L_{10} = (L_i^{-1.11} + L_o^{-1.11})^{-0.9} \quad \text{Eq. 24}$$

III. RESULTS AND DISCUSSIONS

This section presents the numerical analysis of ball bearing performance across varying loads and speeds for three materials: alloy steels, nickel-based superalloys, and titanium alloys. Key performance indicators—load-deflection constants, normal contact load, and fatigue life—were examined to assess structural integrity and reliability.

3.1. Load-deflection constants of ball bearing inner raceway for different materials

The load-deflection behaviour of the bearing inner raceway at 10,000 RPM was examined for three materials: alloy steels, nickel-based superalloys, and titanium alloys, Fig. 3. Alloy steels demonstrated the highest stiffness values, increasing from 2,903,646 N/mm² at zero load to 2,910,913 N/mm² at 47,500 N. Nickel-based superalloys followed a similar but slightly lower trend, rising from 2,800,628 to 2,807,648 N/mm². Titanium alloys exhibited the lowest load-deflection constants, increasing modestly from 1,584,934 to 1,588,994 N/mm² across the same load range. All materials showed a positive correlation between applied load and deflection resistance, with alloy steels showing the steepest increase, indicating better performance under high-load conditions.

Additionally, at a constant applied load of 40,000 N, the effect of rotational speed on stiffness was assessed. As speed increased from 6,000 to 15,000 RPM, a slight reduction in the load-deflection constant was observed across all materials. Alloy steels decreased from 2,911,797 to 2,908,479 N/mm², nickel-based superalloys from 2,808,498 to 2,805,297 N/mm², and titanium alloys from 1,589,462 to 1,587,643 N/mm². Although the changes were relatively minor, they suggest that higher speeds can reduce structural stiffness slightly—most notably in alloy steels—due to dynamic effects such as centrifugal forces and potential thermal expansion. This behaviour should be accounted for in the design of high-speed bearing systems.

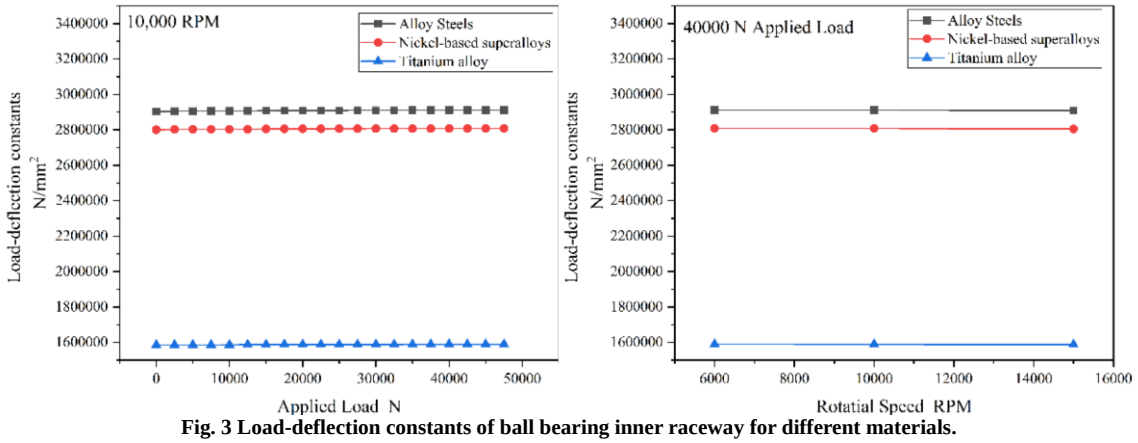


Fig. 3 Load-deflection constants of ball bearing inner raceway for different materials.

3.2. The normal contact load behaviour of the bearing inner raceway for different materials

At a constant rotational speed of 10,000 RPM, the normal contact load on the inner raceway of the bearing was evaluated for alloy steels, nickel-based superalloys, and titanium alloys under applied loads ranging from 0 to 45,000 N, Fig. 4. The results showed a non-linear increase in contact load across all materials as the applied load increased. Alloy steels consistently recorded the highest contact loads, rising from 35.94 N at no load to 3,884.31 N at 45,000 N. Nickel-based superalloys followed closely, ranging from 34.17 N to 3,872.74 N. Titanium alloys had the lowest values, from 16.05 N up to 3,441.17 N. These differences are mainly due to variations in material stiffness and elasticity, with alloy steels exhibiting superior contact resistance, making them more effective at transferring load through the raceway.

For the outer raceway, normal contact load was evaluated at a fixed applied load of 40,000 N, across rotational speeds of 6,000, 10,000, and 15,000 RPM. An increase in contact load with speed was observed in all materials. Alloy steels showed the highest values, increasing from 3,812.24 N to 4,124.77 N.

Nickel-based superalloys followed a similar trend, from 3,687.92 N to 4,004.24 N, while titanium alloys showed the lowest range, from 2,153.25 N to 2,404.37 N. These results suggest that higher speeds intensify dynamic effects—such as centrifugal force and vibration—which in turn raise the contact pressure on the outer raceway. Overall, alloy steels proved most capable of withstanding elevated contact loads, reinforcing their suitability for high-speed, high load bearing applications.

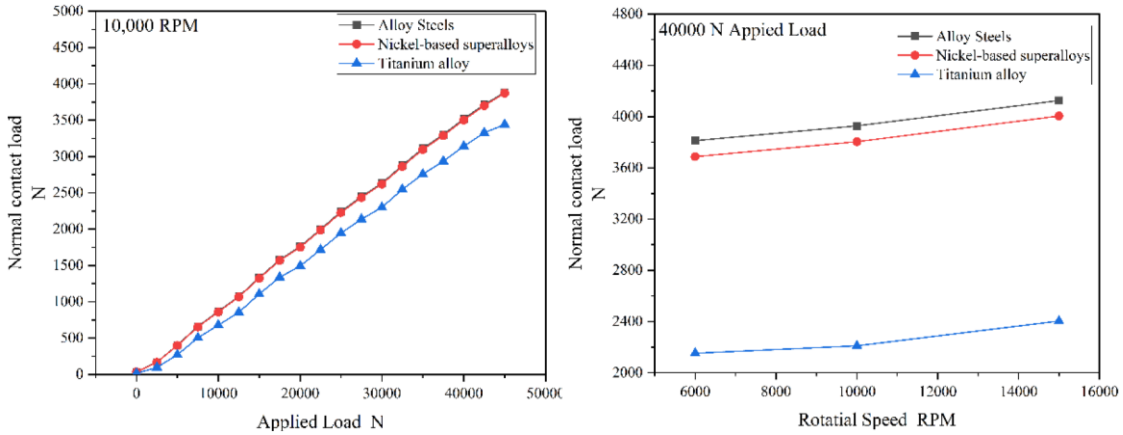


Fig. 4 The normal contact load behaviour of the bearing inner raceway for different materials.

3.3. The fatigue life behaviour of the bearing across different materials

The fatigue life of the bearing at a constant speed of 10,000 RPM was evaluated under increasing applied loads for three materials: alloy steels, nickel-based superalloys, and titanium alloys. Across all materials, fatigue life decreased significantly with rising load, consistent with the inverse relationship between load intensity and bearing longevity, Fig. 5. At zero load, titanium alloys showed the longest fatigue life, approximately 95.4 billion cycles, compared to 20.4 billion and 18.7 billion cycles for nickel-based superalloys and alloy steels, respectively. However, titanium alloys also exhibited the steepest decline in fatigue life as load increased—falling to ~65.1 million cycles at 40,000 N—indicating a higher sensitivity to loading. In contrast, alloy steels and nickel-based superalloys showed more consistent fatigue life trends across the load range, ending at ~42.6 million and ~43.6 million cycles, respectively, under the same load. These results suggest that while titanium alloys offer superior performance under light loads, alloy steels and superalloys are more reliable for heavy-duty applications.

At a fixed 40,000 N load, fatigue life was also analysed across rotational speeds of 6,000, 10,000, and 15,000 RPM. All materials experienced reduced fatigue life with increasing speed, due to enhanced dynamic and thermal stresses. Titanium alloys maintained the highest fatigue life at each speed, decreasing from 1.81 billion to 1.41 billion cycles. Nickel-based superalloys followed, dropping from 360.4 million to 305.9 million cycles, while alloy steels showed the lowest fatigue values, declining from 326.3 million to 279.9 million cycles. These results affirm titanium's excellent high-speed endurance, though its sharp degradation rate must be considered. Meanwhile, alloy steels and superalloys provide steadier, more predictable fatigue performance under varying speed conditions, making them practical for high-speed, high-load bearing systems requiring consistent service life.

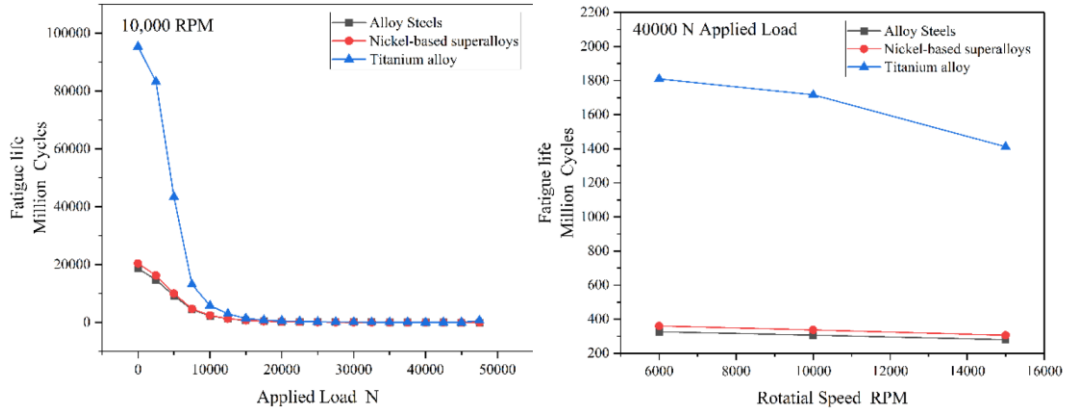


Fig. 5 The fatigue life behaviour of the bearing across different materials.

IV. CONCLUSION

The comprehensive analysis of bearing materials under dynamic loading conditions has revealed critical performance differences. Alloy steels, with their high stiffness and consistent load-deflection behaviour, are best suited for applications demanding minimal deformation and high structural rigidity. Nickel-based superalloys offer a balanced performance with moderate stiffness and fatigue life, making them suitable for high-temperature or aerospace environments.

Titanium alloys, although less stiff, provide exceptional fatigue life at low to moderate loads, positioning them well for lightweight, low-load systems. As rotational speed increases, all materials experience reduced fatigue life and increased contact loads, emphasizing the need for careful material selection based on both operational speed and loading conditions. Overall, the results support the strategic use of each material depending on the specific performance priorities of stiffness, fatigue resistance, or weight efficiency in bearing design.

REFERENCES

[1] R. Rejith, D. Kesavan, P. Chakravarthy, and S. V. S. Narayana Murty, "Bearings for aerospace applications," Tribology International, vol. 181, p. 108312, 2023/03/01/ 2023, doi: https://doi.org/10.1016/j.triboint.2023.108312.

[2] Z. Yang, B. Li, and T. Yu, "Influence of structural parameters and tolerance on stiffness of high-speed ball bearings," International Journal of Precision Engineering and Manufacturing, vol. 17, no. 11, pp. 1493–1501, 2016/11/01 2016, doi: https://doi.org/10.1007/s12541-016-0175-9.

[3] D. K. Ganji and G. Rajyalakshmi, "Influence of Alloying Compositions on the Properties of Nickel-Based Superalloys: A Review," in Recent Advances in Mechanical Engineering, Singapore, H. Kumar and P. K. Jain, Eds., 2020// 2020: Springer Singapore, pp. 537–555, doi: https://doi.org/10.1007/978-981-15-1071-7_44.

[4] S. Gao, L. Wang, and Y. Zhang, "Modeling and dynamic characteristic analysis of high speed angular contact ball bearing with variable clearance," Tribology International, vol. 182, p. 108330, 2023/04/01/ 2023, doi: https://doi.org/10.1016/j.triboint.2023.108330.

[5] T. A. Harris and M. N. Kotzalas, Rolling bearing analysis-2 volume set. Crc Press, 2006 doi: https://doi.org/10.1201/9781482275148.

[6] S. Gao, S. Chatterton, L. Naldi, and P. Pennacchi, "Ball bearing skidding and over-skidding in large-scale angular contact ball bearings: Nonlinear dynamic model with thermal effects and experimental results," Mechanical Systems and Signal Processing, vol. 147, p. 107120, 2021/01/15/ 2021, doi: https://doi.org/10.1016/j.ymssp.2020.107120.

[7] G. Lundberg and A. Palmgren, "Dynamic capacity of rolling bearings," 1949, doi: https://doi.org/10.1115/1.4009930.

★★★